Dengue virus suppression by 25-hydroxycholesterol is mediated by a combination of membrane fusion inhibition, innate immune activation and cholesterol biosynthesis dysregulation

Debayani Chakraborty[1,2], Achinta Sannigrahi[1#], Mahammed Kaif [1,3], Arijit Patra [1], Deep Thakkar[4], Rahul Roy[1,3]

Affiliations:

1 Department of Chemical Engineering, Indian Institute of Science, Bangalore, India

2 University of Trans-Disciplinary Health Sciences and Technology, Bangalore, India

3 Department of Bioengineering, Indian Institute of Science, Bangalore, India

4 Department of Chemical Engineering, Indian Institute of Technology, Gandhinagar, India

#current address: University of Texas Southwestern medical center, Dallas, Texas-75390

Corresponding Author: debayanic@iisc.ac.in, rahulroy@iisc.ac.in

Abstract:

Dengue virus, and other viral pathogens such as SARS-CoV-2 and Zika, utilize specialized glycoproteins to facilitate the fusion of its lipid membrane with that of the host cell, a critical step for viral entry and infection. This membrane fusion process is significantly influenced by factors such as host cell membrane lipid composition, membrane architecture, and cell surface receptors. However, the specific mechanisms by which dengue virus membrane fusion is modulated by the cell membrane lipids are not fully elucidated. We investigate the role of oxidised cholesterol metabolite, 25-hydroxycholesterol (25-HC) in inhibiting dengue virus infection using virus fusion and viral infection assays. We demonstrate that 25-HC significantly impedes the membrane fusion capability of the dengue virus, thereby inhibiting viral entry and infection in cell cultures. Apart from inhibiting membrane fusion, pre-exposure to 25-HC upregulates *CH25H* which inhibits virus growth. Indeed, *CH25H* gene is upregulated along with other ISGs in various cell types as a defence response to dengue virus infection. These insights into the modulation of dengue virus membrane fusion by lipid cofactors in the host cell membrane present a promising avenue for the development of strategies aimed at inhibiting viral membrane fusion, thereby potentially curtailing the spread of the infection. For example, we show that other inhibitors that target mechanisms distinct from 25-HC action on membrane fusion display strong positive synergy in virus inhibition with 25-HC.

Keywords

Dengue virus, 25-hydroxycholesterol, Synergy, Membrane Fusion, Cholesterol homeostasis, Immune activation

Introduction:

Viral membrane fusion is a critical step in the life cycle of enveloped viruses, enabling the delivery of viral genetic material into host cells and initiating infection [1]. These glycoproteins undergo conformational changes to facilitate the merging of the viral envelope with the host cell membrane [2]. For instance, the envelope (E) glycoprotein of Zika virus, as well as the spike (S) glycoprotein of SARS-CoV-2, play pivotal roles in orchestrating membrane fusion by interacting with host cell receptors and triggering fusion at the plasma membrane or within endosomal compartments [3], [4], [5], [6], [7].

Apart from the viral glycoproteins, host cell membrane lipids can significantly influence the efficiency and dynamics of viral fusion. Cholesterol, sphingolipids, and other lipid components of the host membrane modulate the biophysical properties of the fusion site, such as membrane curvature and fluidity, which are critical for successful viral entry [8],[9], [10]. The interplay between viral glycoproteins and host membrane lipids underscores the complexity of the fusion process and highlights potential avenues that can be exploited for antiviral strategies. Although there is currently no specific antiviral therapy approved for dengue, the concept of combination therapy which are being explored for treating viruses like HIV, hepatitis C, and COVID-19 is believed to be employed in dengue infection. Elucidating the role of cofactors in dengue virus fusion is pivotal for advancing antiviral therapeutic development.

Among the host-derived factors with antiviral potential, 25-hydroxycholesterol (25-HC) displays potent activity against a broad range of enveloped viruses [11], [12], [13], [14] and even non-enveloped viruses like Human Rotavirus [15]. Produced by the enzyme cholesterol 25-hydroxylase (*CH25H*) in response to interferon signalling, 25-HC has been shown to inhibit viral entry by altering the lipid composition of host membranes and disrupting the entry process [16], [17], [15].

Beyond its direct antiviral activity, 25-HC also acts as an immunomodulator, influencing the expression of inflammatory cytokines and regulating cholesterol metabolism to limit viral replication [18]. For instance, 25-HC has been shown to inhibit the activation of nuclear factor kappa B (NF-κB), a key transcription factor involved in the expression of inflammatory cytokines such as interleukin-6 (IL-6) and tumour necrosis factor-alpha (TNF-α) [19]. By dampening excessive inflammation, 25-HC helps to prevent tissue damage during

viral infections, thereby contributing to immune homeostasis [20]. Additionally, 25-HC modulates the type I IFN response, enhancing the antiviral state of cells while simultaneously limiting overactivation of the immune system, which could lead to immunopathologic [21]. Another critical aspect of 25-HC's immunomodulatory role is its regulation of cholesterol metabolism, which is tightly linked to immune function. Recent findings show that 25HC enhances innate immunity against bacterial infections by mobilizing accessible cholesterol on the cell surface. Cellular cholesterol is distributed in different pools—like free and sphingomyelin-bound cholesterol—mainly in the plasma membrane and ER. Cholesterol synthesis is controlled by ER transmembrane proteins. When plasma membrane cholesterol is high, accessible cholesterol moves to the ER, where *SCAP* binds it, forming a *SCAP-Insig* complex that inhibits *SREBP* activation and lipid synthesis [22], [23]. In low cholesterol conditions, this complex formation is blocked, allowing the *SCAP-SREBP* complex to move to the Golgi and trigger cholesterol production. ACAT also regulates accessible cholesterol by converting it into esterified cholesterol for storage in lipid droplets [24].

By reducing cholesterol synthesis and uptake through the suppression of sterol regulatory element-binding protein (*SREBP*) activity, 25-HC limits the availability of cholesterol required for viral replication and assembly [25]. This dual immunomodulatory role of 25-HC—modulating lipid metabolism and immune signalling—ensures that the host cell environment is less conducive to viral propagation while maintaining an effective immune response. Although the antiviral effect of 25-hydroxycholesterol (25-HC) has been extensively studied across various viral infections, its multifaced role in modulating Dengue virus infection has not yet been fully elucidated.

Given the promising antiviral activity of 25-HC, we hypothesize that it disrupts DENV membrane fusion by targeting the conformational changes of the E protein. This study aims to (1) elucidate the mechanism of 25-HC action, and (2) assess the synergistic effects of 25-HC with established antivirals. We evaluated whether 25-HC enhances antiviral potency and reduces the effective dosage of individual drugs, thus offering a potential strategy for more effective therapeutic interventions against DENV infection [26].

In this study, we investigated the mechanism of action of 25-hydroxycholesterol (25-HC) and major gene expression changes in response to dengue virus infection influenced by 25-HC pre-treatment. To assess the mechanism of action of 25-Hydroxy cholesterol in its known concentration can exhibit enhancement of antiviral potency lowering the dosage of individual

drugs, we evaluated whether there is a synergistic relationship with some known anti-virals in the context to determine if the combination of two compounds can enhance the efficacy compared to using them individually. Here we present the inhibitory role of 25-HC which contributes to multiple facets in DENV infection landscape. First, 25-HC reduces the binding of enveloped E protein with lipid membrane thus inhibiting the Capsid-target membrane association and subsequent fusion event. Second, 25-HC treatment attenuates the cholesterol synthesis gene expressions eventually manipulating the total cholesterol homeostasis in DENV infected cells. Third, 25-HC activates key inflammatory and immune response genes prompting the host cell innate immune activation against the infection. Our findings not only uncovered the molecular mechanisms of 25-HC induced DENV inhibition but also founded the premise for potential antiviral development which is also evident from our study on synergism between 25-HC and broad-spectrum antivirals.

Materials and Method:

Cell Culture: BHK-21 (ATCC CRL-1587), Vero E6 (ATCC CRL-1587), RAW 264.7 (ATCC TIB-71), Huh-7 (a generous gift from Dr. Soumitra Das) cells were maintained in Dulbecco's Modified Eagle Medium (DMEM, Gibco Thermo-Fisher Scientific), supplemented with 10% fetal bovine serum (Thermo-Fisher Scientific), 15 mM HEPES, 200 mM glutamine, 100 mM non-essential amino acids, and penicillin-streptomycin 100 U/ml at 37°C, 5% CO_2.

Virus production: The plasmid pFK-DV encoding a synthetic copy of full-length genomic sequence DENV2 strain 16681 was a gift from Dr. Ralf Bartenschlager and was used to generate the Dengue virus as previously reported [27]. Briefly, viral RNA was synthesized from the linearized plasmid by in vitro transcription (HiScribeTM SP6 RNA Synthesis Kit) followed by capping. RNA was purified by Sodium-acetate precipitation and transfected to the BHK cells by lipofectamine Messenger-Max (Thermo-Fisher Scientific) and the supernatant containing infectious virus was harvested and cleared from the cell debris by low-speed centrifugation. Passage 1 (P1) virus was produced by infecting Vero E6 cells with the supernatant collected above. The virus particles were collected and purified from cell debris by low-speed centrifugation. This supernatant containing P1 virus was further used for infecting cells in the presence or absence of different concentrations of 25-hydroxycholesterol.

Determination of viral infectivity and calculation of viral load:

Focus Forming Unit (FFU) Assay:

Approximately 0.05 × 10^6 Vero E6 cells were seeded in 24 well plates to grow and reach a confluency of 70%. Cells were then infected with serial threefold dilutions of Dengue Virus and incubated for 1 hour at 37°C to allow adsorption. The inoculum was then removed and the cells were overlaid with 1.5% carboxymethylcellulose (CMC) in DMEM supplemented with 2% FBS. After 48 of incubation, cells were fixed with 4% paraformaldehyde and permeabilized with 0.1% Triton X-100. Infected foci were detected using a virus-specific primary antibody 4G2 with 1:500 dilution (Catalog No. GTX57154) and secondary antibody of Goat anti-Mouse IgG (H+L) Cross-Adsorbed Secondary Antibody, Alexa Fluor™ 488(Catalog No- A-11001) with the concentration of 1 µg/mL. The cluster of the infected cells (focus) was captured under an inverted microscope (Evos M7000 automated imaging system) by taking 100 images from the center, combining them into a single merged image

Quantification of Dengue Virus Genomic RNA:

To quantify Dengue virus genomic RNA from cell culture supernatants, viral particles were first concentrated using polyethylene glycol 8000 precipitation, followed by resuspension in Tricine buffer (20 mM Tricine, pH 7.8, 140 mM NaCl, and 0.005% Pluronic F-127). Total RNA was extracted using RNAiso Plus reagent (Takara, Cat. No. 9108/9109) according to the manufacturer's instructions. Complementary DNA (cDNA) synthesis was performed using SuperScript™ IV Reverse Transcriptase (Thermo Fisher Scientific, Cat. No. 18090010) with random hexamer primers. For quantitative PCR, 100 ng of cDNA was amplified using Phusion High-Fidelity DNA Polymerase (NEB, Cat. No. M0530S), 10 µM each of forward (5′-GTCCCCTTCTCAGGCAGAATGAGCC-3′) and reverse (5′-GTTCGTGTCTCCAGTCCCATTCCC-3′) primers, and EvaGreen dye in a 1× reaction buffer. PCR was carried out for 45 cycles (15 seconds at 98°C and 15 seconds at 58°C). Viral genome copy number was calculated using a standard curve generated from serial dilutions of a plasmid containing the full-length DENV2 genomic sequence.

Time of Addition Assay:

For the FFU assay, approximately 0.05×10^6 Vero cells were seeded in 24-well plates and cultured to ~70% confluency. For genomic RNA quantification, ~0.3×10^6 Vero cells were seeded in 6-well plates and grown to a similar confluency. Cells were either pre-treated with

25-hydroxycholesterol (25-HC) for varying durations or infected with dengue virus at a multiplicity of infection (MOI) of 0.5, followed by post-infection treatment with 25-HC (as per the FFU assay protocol described above). For viral genomic RNA quantification, cells were treated with 25-HC either prior to or following infection with dengue virus at MOIs of 0.5 or 5. Viral genome copy number was determined as described in the quantitative PCR section above.

Counting of Focus Forming Units and size of the Focus Forming Units:

Green fluorescence from the GFP channel, indicative of viral infection, was used to quantify the number of foci-forming units. Images were processed using auto-generated code that implemented a minimum pixel size threshold to identify and select objects, followed by the creation of a mask. Refinement steps included dilation, erosion, opening, and closing operations, with all parameters standardized and consistently applied across all images. The code is available at [https://github.com/Debayani12/25HC].

mRNA sequencing of Raw 264.7 cells: RAW 264.7 cells (ATCC TIB-71) were cultured in Dulbecco's Modified Eagle Medium (DMEM) supplemented with 10% fetal bovine serum (FBS) and 1% penicillin-streptomycin at 37°C in a humidified atmosphere containing 5% CO_2. Cells were seeded at a density of 0.1 x 10^6 cells in 6-well plates prior to the day of experiment and treated with 1 µM 25-HC for eight hours, followed by wash and DENV infection for 24 hours. After treatment, cells were washed with PBS and lysed with TRIzol reagent (Invitrogen). mRNA libraries were sequenced using Illumina NovaSeq X plus (By company Med genome) to generate 2x150bp reads/sample.

Data Analysis:

The raw RNA-seq reads were trimmed to remove adapter sequences and low-quality bases (Phred score < 20) using Trim Galore! [https://www.bioinformatics.babraham.ac.uk/projects/trim_galore/]. Quality assessment of the trimmed reads was performed using FastQC [http://www.bioinformatics.babraham.ac.uk/projects/fastqc/].

The reference genome and annotation were downloaded from ensembl.org. The raw reads were aligned to reference with STAR aligner [28] with default parameters. The aligned reads were counted per gene with feature Counts in paired-end mode at gene meta feature level

[29]. Multimapping reads were not counted. After counting, PyDESeq2 [30], a python implementation of popular R package DESeq2 was used for differential gene expression analysis. Genes with adjusted p-value of less than 0.01 and absolute $\log_2$FoldChange greater than 1 were considered as differentially expressed genes. These genes were used as input for statistical overrepresentation test for gene ontology with PantherDB [10.1038/75556, 10.1093/genetics/iyad031, 10.1002/pro.4218]. All genes that had at least 1 count in any sample were used as background list for the test. FDR correction was used to correct for multiple testing.

Calculation of Synergy:

Approximately 0.05×10^6 Vero-E6 and 0.04×10^6 BHK-21 cells were seeded in 24-well plate and waited up to 70% confluency.

To evaluate drug synergy, we performed checkerboard assays wherein combinations of two antiviral compounds such as Chloroquine (Sigma-C6628-25G), Picolinic acid (Sigma-P42800), remdesivir (MedChem-HY-104077) and K-22 (N-{3-[4-(4-bromophenyl)-4-hydroxypiperidin-1-yl]-3-oxo-1-phenylprop-1-en-2-yl}benzamide) (Chemdiv 4295-0370) (were tested across a matrix of concentrations below their respective IC_{50} values. Vero E6 (and BHK-21 in the case of chloroquine) cells were seeded in 24-well plates as above-mentioned counts to ~70 % confluency and treated with varying concentrations of each compound alone and in combination, 3×3 matrix format for 4 hours, followed by infection with dengue virus (DENV). After 48 hours of incubation at 37 °C with 5% CO_2, culture supernatants were collected, and viral RNA levels were quantified using qPCR. The percentage inhibition (efficacy) at each concentration was calculated using the formula:

$$\varepsilon = (\varepsilon_{max} \times (D / IC_{50})^m) / (1 + (D / IC_{50})^m)$$

where ε_{max} is the maximum observed efficacy, D is the drug concentration, IC_{50} is the half-maximal inhibitory concentration, and m is the Hill slope. Using the IC_{50} and E_{max} values derived from virus copy number reduction assays, we computed the expected additive effect of the two drugs under the Bliss independence model:

$$\varepsilon^B = \varepsilon_1 + \varepsilon_2 - (\varepsilon_1 \times \varepsilon_2) / 100$$

The observed combined efficacy (ε_comb) was compared against ε_B to calculate Bliss synergy (S_B = ε_comb - ε_B) and the Bliss synergy ratio (α = ε_comb / ε_B). An additional

mechanistic model was employed to estimate the interaction coefficient (α) using the rearranged combination efficacy formula that accounts for modified IC_{50} values in the presence of interacting drugs. These calculations were performed using custom Python scripts, enabling parameter fitting and synergy quantification. For independent validation, we also calculated the synergy score as $S = Y_c / (Y_1 \times Y_2)$, where Y_c is the relative viral RNA reduction with the drug combination, and Y1 and Y2 are reductions observed with each drug alone. A value of $S < 1$ was considered indicative of positive synergy.

For each combination, IC_{50} and E_{max} values were calculated individually, followed by Bliss synergy and α value were calculated with code available at [https://github.com/Debayani12/25HC].

Cell Viability (MTT) Assay:

Cell viability was assessed using the MTT assay. Briefly, Vero cells were seeded in 96-well plates at a density of 1*10^4 cells/well and treated with the indicated concentrations of 25-hydroxycholesterol for 24 hours. Following treatment, 10 µL of MTT reagent (5 mg/mL in PBS; Thermo-Fisher Scientific-M6494) was added to each well and incubated at 37°C for 3-4 hours. The resulting formazan crystals were solubilized using 100 µL of DMSO, and absorbance was measured at 570 nm using a microplate reader. Cell viability was expressed as a percentage relative to untreated controls.

Preparation of labelled virus for fluorescence dequenching assay: The virus supernatant was collected 72 hours after the infection, and the virions were pelleted by ultracentrifugation at 4 °C for 15 hours for 30000 g. The virus pellet was resuspended in a buffer containing 20 mM Tricine (N-(2-Hydroxy-1,1 bis (hydroxymethyl)ethyl) glycine) pH 7.8, 140 mM NaCl and 0.005% Pluronic F-127 (Tricine buffer) and 500 nM DiD as described previously [31]. The virus was further purified over an Opti-prep density gradient (32000 rpm at 4°C for 3 hours) with 15%, 25%, 40% and 60% density levels. The band between 25% and 40% was harvested, aliquoted, and stored at –80°C. Before the experiment, the virus was collected and cleared from Opti-prep using a 100 kDa filter (Amicon ultra 100 kDa centrifugal filter unit). The DiD-labeled viruses was stored at 4°C and was used within 2 days for the dequenching assay.

Labelled Virus Infection Assay: Vero E6 cells were seeded in 8 well chambered coverslip and either treated with different concentrations of 25-HC for four hours or without pre-treatment, washed, kept on ice for 10 minutes and infected with 5 MOI of DiD labelled virus

for one 1.5 h at 37 °C. The virus inoculum was then removed, fixed with 4% paraformaldehyde (PFA) and incubated with DAPI, washed and finally mounted on glass slide. Images were acquired using Andor Dragonfly confocal microscope. Quantification of the virus relative to the DAPI positive cell was quantified using ImageJ/Fiji software. Control

Calcein entrapped liposome Preparation: Calcein entrapped liposomes were made based on previously used protocol [32], [33]**.** Briefly, lipids were mixed in chloroform that was made to evaporate under nitrogen to form a thin film in the glass vial. Residual chloroform was made to evaporate by keeping the samples in vacuum overnight. The lipid films were then hydrated in PBS, or fluorescent dye calcein (80 mM) in phosphate buffer saline (PBS) or SYTO RNA Select (10 μM). The lipid suspension at final lipid concentration of 1mM was then subjected to sonication and removal of extra dye by dialysis membrane (Snakeskin Dialysis, 3.5 K, Thermo-Fisher). Small Uni-lamellar Vesicles (SUV) were prepared with the lipid composition of POPC:SM:CH: POPG as 1:1:1:1 was used to compare fusion with Liposomes with the composition of POPC:SM:CH: HC: POPG at a ratio of 1:1:0.5:0.5:1 to measure the role of 25-HC in most of the assays. Liposomes were also prepared in varying concentrations of 25-HC, altering cholesterol. Liposomes were prepared at pH 5 and 7.5 respectively.

Quantification of virus fusion by Content Mixing assay: Liposomes were prepared with the lipid composition of POPC:SM:CH:POPG as 1:1:1:1 and POPC:SM:CH: HC: POPG at a ratio of 1:1:0.5:0.5:1 containing an RNA binding dye, SYTO RNA-Select (10 μM) or fluorescent dye calcein (80 μM) in phosphate buffer saline (PBS) in pH 5 and 7.5 respectively. Liposomes prepared were composed of varying concentrations of 25-hydroxycholesterol: Cholesterol as 0.5 and 0.5 respectively. The lipid suspension was subjected to bath sonication to form Small Uni-lamellar vesicles. The excess unincorporated dye was removed by dialysis membrane (Snakeskin Dialysis, 3.5 K, Thermo-Fisher). RNA from the In-vitro transcription mentioned above was re-suspended in RNAase-free water 1 ug of RNA was added to the RNA binding dye and the change in absorbance was recorded. Change in Fluorescence was measured by Fluorescence Spectrometer (Agilent) with absorption/emission maxima set at ~490/530 nm. Fusion analysis by RNA genome exposure was performed by the following formula where F equals the difference between Final intensity (A_i) and Initial intensity(A_0) of reference IVT RNA, divided by the difference between final (R_i) and initial absorbance (R_0) of test virus, then multiplied by 100.

$F=(A_i-A_0)/(R_i-R_0) *100$

For calcein leakage assay, calcein-tagged liposomes were added into the cuvette, and change in intensity was recorded by excitation/emission in 495 and 515 nm respectively, starting from the baseline (I_0), followed by pausing the recording and addition of 5 ul of virus (10 times dilution from stock) and mixing the contents properly (I_t). After a certain time, 1% TritonX was added to achieve complete dequenching of the dye (I_{max}). The extent of liposome content leakage and membrane mixing was measured as the ratio of dequenching as

Dequenching= $(I_t - I_0)/(I_{max} - I_0) \times 100$

FRET-based virus and liposome fusion Assay: We also developed a FRET-based fusion assay and compared membrane fusion with the target membrane in the presence and absence of 25-hydroxycholesterol. The virus liposome fusion was also monitored by preparing liposomes having lipid conjugated FRET pair Rhodamine (RHO) and Nitrobenzoxadiazole (NBD) with the lipid composition of POPC:POPG:CH:SM:NBD:RHO as 1:1:1:1:0.01:0.01 and POPC:POPG:CH:25-HC:SM:NBD:RHO as 1:1:0.5:0.5:1:0.01:0.01prepared in pH 5 and pH 7.5 respectively. A liposome fusion reaction was performed on a fluorescence spectrophotometer with excitation and emission wavelengths as 467 nm and 590 nm. 95 ul of the liposome was added into the cuvette (F_0) followed by the addition of virus (F_1) and 1% TritonX respectively. Full fusion was measured as a function of the decrease of the acceptor fluorescence (Rhodamine) signal due to fusion. Signals were normalized to the lowest fluorescence produced by the detergent solubilization and the fusion curves were plotted as a percentage of fusion efficiency considering maximum fusion efficiency with 1% TritonX 100 as 100%(F_{max}).

Fusion Efficiency= $(F_0 - F_1)/(F_0 - F_{max}) \times 100$

Virus Binding Assay in-vitro: Multilamellar vesicles (MLVs) were prepared using the thin-film hydration method. Briefly, lipids consisting of composition of POPC:SM:CH:POPG as 1:1:1:1 and POPC:SM:CH:HC:POPG at a ratio of 1:1:0.5:0.5:1 dissolved in chloroform, followed by evaporation of the solvent to form a thin lipid film on the inner wall of a round-bottom flask. Residual solvent was removed under high vacuum overnight. The resulting lipid film was hydrated with PBS solution at final lipid concentration of 1mM, with periodic vortexing, to yield multilamellar vesicles. The MLVs were subsequently equilibrated at room temperature before further use or characterization.

For lipid–protein binding analysis, 300 µL of 1 mM multilamellar vesicles (MLVs) were incubated with dengue virus envelope protein (final protein concentration of 5 µM) at 37°C

for 30 minutes with gentle mixing. Following incubation, the vesicle–protein suspension was centrifuged at 22,000 × g for 30 minutes to separate bound and unbound proteins. The supernatant was carefully collected, and the pellet was resuspended in 300 µL phosphate-buffered saline (PBS). Both fractions (supernatant and pellet) were analysed separately by SDS-PAGE to determine protein distribution. The gel was stained with Coomassie Brilliant Blue to visualize protein bands and to identify the fraction in which the dengue virus envelope protein was enriched.

RESULTS

DENV2 inhibition by 25-hydroxycholesterol (25-HC)

To investigate the antiviral properties of 25-HC on Dengue virus, we measured the genomic copy number of DENV2 after 48 hours post-infection in the presence and absence of 25-HC. To limit 25-HC cytotoxicity, we measured and verified the CC50 value (~179.8 μM) of 25-HC on Vero cells (Figure S1D) and did not employ higher than 10% this concentration. We found that pre-treatment with 25-HC (for 8 hrs before infection) reduces Dengue viral RNA (measured at 48 hours post infection (hpi)) in a 25-HC concentration-dependent manner with up to1800-fold reduction at the highest concentration tested (at 10 μM 25-HC with 0.5 MOI) (Figure 1A). A similar inhibition trend was observed at higher MOI (5 MOI) with up to 50-fold reduction (at 10 μM of 25-HC) as well as in BHK cells (100-foldreduction at 10 μM with 0.5 MOI). This suggests that 25-HC is a potent antiviral against Dengue virus as reported for other Flaviviruses [34]. However, this inhibition was significantly reduced in Vero cells (by ~ one log order at all concentrations) when 25-HC is added post infection (8 hpi) suggesting that virus entry inhibition is a key mechanism for 25-HC action (Figure 1A).

To further confirm that 25-HC acts by attenuating viral entry, we examined Dengue infection in presence of 25-HC using time of addition assays. When we compared the Focus Forming Units (FFU) of Dengue virus after 8 hrs of pre-incubation with 25-HC (1 μM), we observed a dramatic drop in infectivity as observed by the reduction in FFUs (Figure 1B and 1C).A significant inhibition is observed even when 25-HC exposure is limited to 1 hr and the cells have been allowed to recover for 7 hours before infection with Dengue virus (Figures1B and 1C). Since the cells were washed with media to replace free 25-HC in the FFU experiments, we attribute the observed virus inhibition is promoted by cell-membrane bound 25-HC. However, the inhibition by 25-HC is markedly reduced when it is added to the cells after post infection consistent with viral RNA measurements (Figure 1C and 1D). Indeed, longer delays in addition of 25-HC continues to reduce its efficacy further confirming that 25-HC is predominantly an early lifecycle inhibitor (Figure 1C and 1D). When 25-HC was added closer to the infection, FFUs sizes did not vary significantly from the untreated control FFU suggesting that replicative fitness of the virus is not perturbed significantly and the cell entry inhibition is the major mechanism of action.

However, when 25-HC was pre-treated for a limited time (1 hour) before Dengue infection, we observed a marked (> 80%) increase in the FFU size suggesting cellular metabolism and

gene expression dysfunction induced by 25-HC mediated signalling can modify the viral replicative fitness in Vero cells (Figure 1B and 1 E). This suggested that the action of 25-HC on controlling Dengue virus infection can be mediated by a combination of inhibition of physical entry and dysregulation of the cellular metabolism.

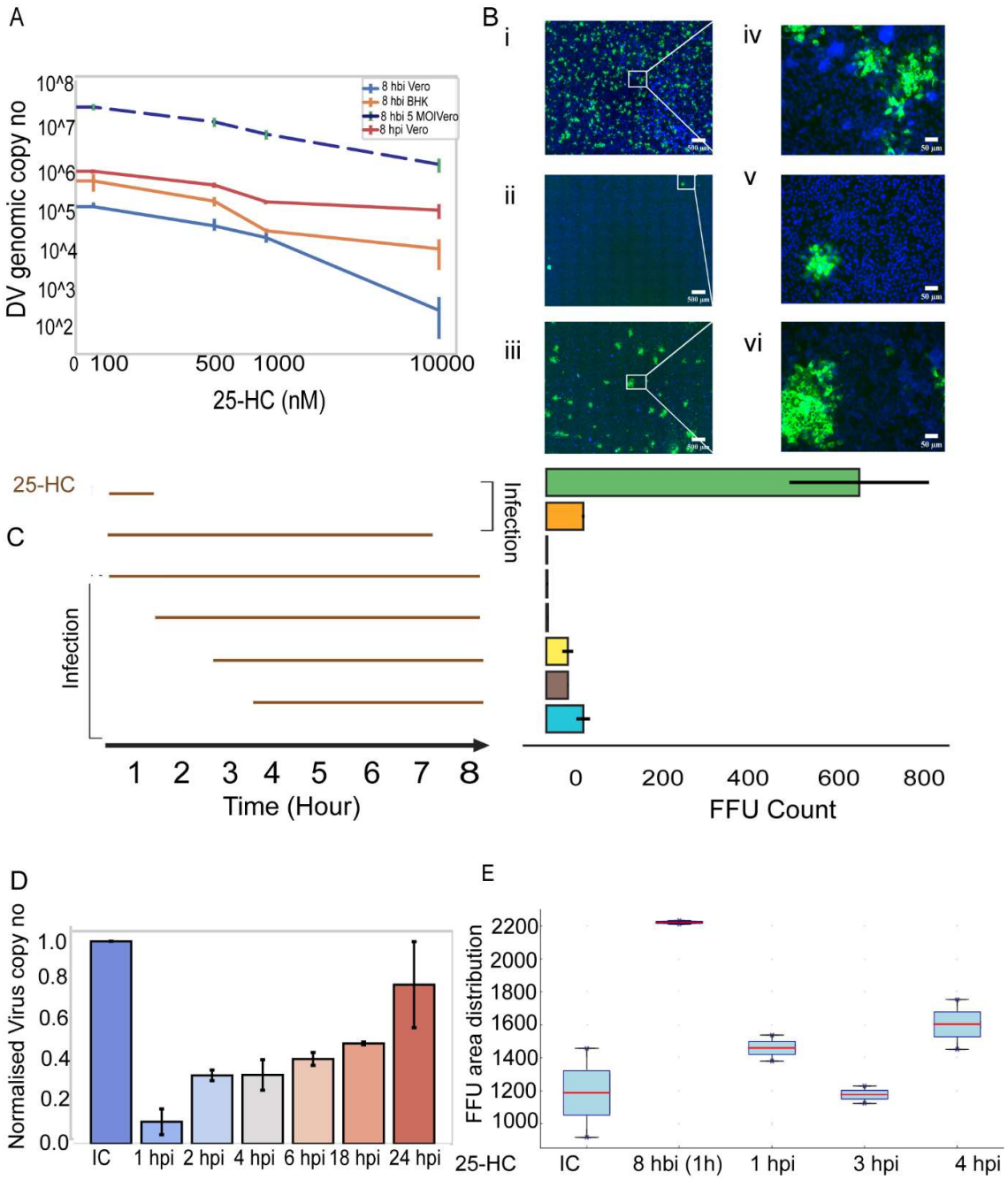

Figure 1: Antiviral activity of 25-hydroxycholesterol (25-HC) against Dengue virus (DENV)

A. Immunofluorescence images showing Focus Forming Units (FFU) in DENV-infected Vero cells, with and without pre-treatment of cells with 25-HC (1 µM) for 1 hour, followed by removal of 25-HC and infection after 7 hours (n=2). Scalebar represents 500 µm. (i) Infection control at 0.05 MOI (ii) 8 hrs of pre-treatment with 25-HC before infection (iii) 1 hr pre-treatment with 25-HC followed 7 hr recovery before infection, (iv), (v) and (vi) are cropped zoomed images of the FFUs corresponding to (i), (ii) and (iii), respectively (scalebar represent50 µm).

B. Time-of-addition FFU assay: Left panel shows the schematic representation of experimental conditions, where Vero cells were treated with 25-HC (1 µM) and infected with DENV at various time points. FFU counts at 48 hours post-infection (hpi) recorded for each treatment (n=2, biological replicates) are shown in the right panel. Data are presented as mean ± SEM.

C. DENV genomic copy numbers (qPCR) measured at 48 hpi with 25-HC added to the cells at different time points post-infection (n=2, biological replicates). Data are presented as mean ± SEM.

D. DENV genomic copy numbers (qPCR) at 48 hours post infection (hpi) in Vero cells treated with varying concentrations of 25-HC under different conditions.

E. Box plots showing FFU area distribution (in pixels) for infection control and infection with 25-HC treatment for different intervals post infection (n=2).

25-hydroxycholesterol inhibits Dengue virus membrane fusion

To elucidate the mechanism of DENV inhibition by 25-HC, we first examined the effect of 25-HC on dengue virus membrane fusion *in vitro*. For this, we prepared fluorescence-based virus liposome membrane fusion assays and tested both lipid mixing and content mixing where we used liposomes with equimolar concentration of POPC, POPG, SM, CH (quaternary control) and liposomes of similar composition altering sterol compositions with varying concentration of 25-HC, keeping total sterol constant. First, we tested virus membrane fusion using the dequenching of the DiD dye. An increase in fluorescence is observed when DiD-labeled virus is mixed with SUVs of quaternary control composition (POPC:SM:CH:POPG at a ratio of 1:1:1:1) only at pH 5 or lower (Figure S3A).When 25-HC is added to the target liposomes, we observed a reduction in fusion fraction in concentration dependent fashion (Figure 2A).There is at least a two-fold decrease in lipid mixing when more than half of the cholesterol from the target membrane is replaced with 25-HC, 12.5% HC composition (POPC:SM:CH:HC:POPG at ratio of 1:1:0.5:0.5:1). To ensure the presence of DiD in virus membrane not perturbing the fusion process, we used lipid attached dye, NBD-PE (donor), Rhodamine PE (acceptor), a FRET pair where energy transfer between

these two dyes can be tracked upon membrane fusion. In the NBD-Rhodamine FRET assay, we also observed an approximately 2-fold decrease in membrane fusion (Figure 2D) when 25-HC was present in the target membrane.

Additionally, we verified content mixing during membrane fusion with two separate assays. First, we used calcein dequencing due to dye leakage from liposomes upon membrane fusion and observed a ~2-fold decrease in membrane disruption (Figure S3B). To further confirmed content mixing, we quantified the level of access to the viral RNA from RNA dye encapsulated in target liposomes [35]. We observed a ~5-fold reduction in content mixing based on genome exposure assay in the presence of 12.5% 25-HC in the target liposome membrane (Figure 2B).

To get a plausible mechanistic insight on the fusion-inhibition process by 25HC, we studied the binding of the envelope protein (E) with model membrane containing different molar fraction of 25-HC as the envelope protein is known as a principal component in virus-target membrane fusion event [5]. Using a sedimentation assay we found that the Envelope protein binds strongly with the quaternary control liposomes (without 25-HC) at low pH as evident from the appearence of a strong band in the membrane bound fraction(pellet) whereas no visible band was observed in the unbound fraction(Supernatant). In contrast, the presence of both 12.5% and 25% HC composition significantly supressed the binding of E-protein with membrane as we did not see anyintense band in the membrane bound fractions (Figure 2F).The insignificant change in the binding phenotypes for 12.5% and 25% 25-HC suggests that 25-HC inclusion in model membrane can reduce the cholesterol accessibilty towards the E protein thus inhibits the fusion event. This observation is in line with the recent reports [36] which showed that accesible pool of cholesterol is ubiquitous in bacterial and viral infections and 25-HC has a crucial role in reduction of accessible cholesterol pool through mobilization from the host cell membrane surface.

To confirm the role of 25-HC in the prevention of binding, we further explored the effect of 25-HC on DENV binding to the cell. During DENV entry, membrane fusion between the virus and host cell occurs within the endosomal compartment, driven by a pH-dependent conformational change in the viral envelope protein [5]. To test this process, we used DiD-labeled virus particles. In their intact state, the DiD signal is quenched; however, upon viral entry, dequenching occurs, leading to an increase in fluorescence intensity. This increase signifies the fusion of viral and endosomal membranes, allowing us to monitor viral fusion by

identifying the rise in fluorescence intensity of the labeled viruses [37] (Figure 2G). We observed that pre-treatment Vero E6 cells with different concentrations of 25-HC for 4 hours did not affect the percentage fusion (Figure 2J) but the total number of DiD labelled virus particles decreased suggesting reduced binding as 25-HC concentration is increased (Figure 2H).

Next, to investigate whether exogenous uptake of 25-hydroxycholesterol could perturb membrane fusion, we pre-incubated either liposomes or the virus with 1 μM 25-hydroxycholesterol and measured membrane fusion using the DiD lipid mixing assay] (Figure 2D). Even in this case, we observed ~25% reduction in membrane fusion when vesicles were pre-incubated with 25-HC (1 μM, 8 hrs),while no significant decrease is observed when the virus was exposed to the same conditions.

Previously, it was reported that negatively charged phospholipid bis(monoacylglycerol)phosphate (BMP) is abundant in late endosomal membranes and is thought to play a role in membrane deformation and the formation of intraluminal vesicles within late endosomes [10]. In this study, we created liposomes containing 25% BMPs and examined membrane fusion where we observed ~4-fold reduction in membrane fusion when 25-hydroxycholesterol was present in the target membrane (Figure 2E) similar to the POPG present in the target membrane.

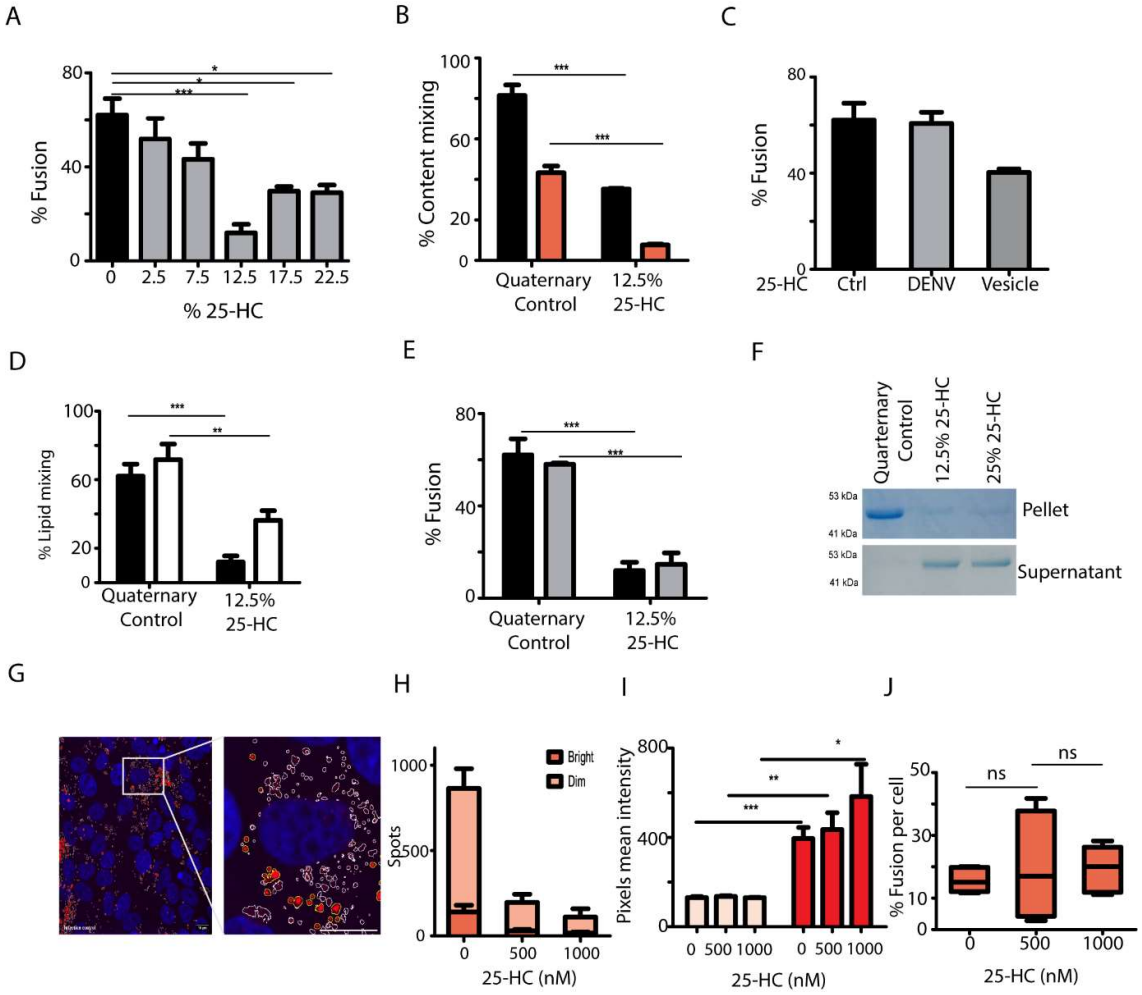

Figure 2: Effect of 25-hydroxycholesterol (25-HC) on membrane fusion *in vitro*

A. Dengue virus (DENV) membrane fusion efficiency as a function of percentage of 25-HC of total lipid composition in the vesicle measured from lipid dye dequenching of DiD-labeled virus at pH 5. Data is presented as mean ± SEM (n=3), with p-values derived from a two-tailed paired t-test (*p ≤ 0.05).

B.Comparison of content mixing quantified through calcein dequenching (black) and viral RNA genome exposure (red) with or without 12.5% 25-HC in vesicles. Data is presented as mean ± SEM (n=3) with p-values derived from a two-tailed paired t-test (*p ≤ 0.05).

C.Comparison of membrane fusion efficiency measured by DiD dequencing when Dengue virus (1 µM for 1 hour) or vesicles (1 µM for 8 hours) is pre-incubated with 25-HC. Data is presented as mean ± SEM (n=3).

D.Comparison of lipid mixing performed by labeling the target membrane with a FRET pair (NBD and Rhodamine, shown as white bars) and DiD dequencing (black bars) with 12.5% 25-HC in the vesicles.

Data are presented as mean ± SEM (n=3), with p-values derived from a two-tailed paired t-test (*p ≤ 0.05).

All the above vesicle (quaternary) controls contained POPC:POPG:SM:CH lipids in 1:1:1:1 ratio.

E. Membrane fusion (DiD dequenching) in the presence of two different anionic lipids (POPG, black and BMP, grey) with 12.5% 25-HC shows similar reduction in fusion efficiency in both cases. Data are presented as mean ± SEM (n=3), with p-values derived from a two-tailed paired t-test (*p ≤ 0.05).

F. SDS-PAGE analysis of a vesicle sedimentation assay shows reduction in DENV2 envelope protein binding to quaternary vesicles with 12.5% and 25% 25-HC at pH 5.

G. Confocal image showing DiD-labeled DENV (red) binding to Vero cells (nucleus in blue, Hoechst). Zoomed images show assignment of bound (yellow circles) and fused (white circles) viral particles based on intensity analysis using ImageJ.

H. Stacked bar chart quantifying total particles per cell (fused viruses in dark orange and bound viruses in light orange) under 25-HC pre-treatment (n=5). Data are presented as mean ± SEM.

I. Mean intensity of bright and dim viral particles quantified from images as shown in G panel (n=5). Data are presented as mean ± SEM.

J. Box plots showing the percentage of fused particles (n=5). The central line marks the median, the box boundaries represent the 25th and 75th percentiles, and whiskers indicate the minimum and maximum values.

Innate immune response with 25-HC exposure in Dengue virus infection

Since Dengue infection of macrophages and dendritic cells has been shown to be modulated, perturbation of the infection by 25-HC can also act to suppress viral infection. As observed in Vero and BHK cells, pre-treatment with 25-HC of macrophages (RAW 264.7 cell line) for eight hours resulted in a six-fold reduction in the intracellular Dengue virus load (infection @5 MOI), suggesting its antiviral activity is not cell type specific (Figure 3A). It is important to note that *CH25H* gene is an interferon-stimulated gene (ISG) responsible for 25-HC biosynthesis and can itself be modified both due to virus infection and/or due to signalling feedback upon 25-HC exposure [11]. We found a significant elevation in *CH25H* expression upon DENV infection across all cell types tested, including Raw 264.7 (~80-fold; Figure 3B), as also observed in the western blot (Figure S7B), Vero (~70-fold; Figure 3C), and BHK (~110-fold; Figure S7A) cells. This suggests *CH25H* gene upregulation is a common feature in DENV infection even in non-immune cell types and is consistent with other flavivirus infection mediated upregulation of CH25H gene [34]. We also found that direct exposure to

only 25-HC is also able to increase *CH25H* mRNA levels suggesting a positive feedback loop wherein 25-HC induces *CH25H* gene expression (Figure 3E). Meanwhile, 25-HC pretreatment before DENV infection led to a decrease in *CH25H* expression compared to infection control, likely due to a reduced infection (Figure 3B,3C).

To test whether specific 25-HC mediated activation or a general innate immune response is sufficient for DENV inhibition, we employed a non-viral activation of the RAW cells followed by DENV infection. For this, RAW cells were pre-treated with lipopolysaccharide (LPS), followed by DENV infection. Again, we observe a marked upregulation of *CH25H* expression in response to LPS treatment. Additionally, LPS treatment significantly reduced viral load, further supporting the role of a broad innate immune response as a mediator of antiviral defence (Figure 3D, 3E).

To examine how 25-HC might control of Dengue virus (DENV) via host cell gene expression regulation, we measured host gene expression changes upon Dengue infection with and without 25-HC with RNA-Seq. As reported previously [38], DENV infection of innate immune cells activates pathways associated with pro-inflammatory response, immune activation, chemotaxis, and stress response (Figure S6 A&B).

The gene expression changes during DENV infection in presence of 25-HC is even more pronounced and we observe dramatic changes in pathways related to adaptive immune responses, inflammatory response and innate immune activation upon virus infection in the presence of 25-HC (Figure 3B& 3C). In particular, we find marked upregulation of key immune and inflammatory response genes such as *NLRP3, Ccl2, CcL7*, and *Csf3* in DENV infected cells pre-treated with 25-HCcompared to the DENV infection (Figure 3C). To identify whether this response is purely due to virus infection or whether 25-HC is perturbing the innate immune response to the virus infection, we compared the gene expression changes between the differences between DENV infected cells in absence and presence of 25-HC (Figure S6 C). The enhanced transcriptional response in the presence of 25-HC aligns with the results of the gene ontology (GO) enrichment analysis, where immune and inflammatory processes are significantly enriched, underscoring the robust activation of the immune system by 25-HC in the case of DENV infection (Figure S6A). 25-HC treatment (at 1μM), however, is not sufficient to perturb the cellular gene expression (Figure S7 D) in isolation suggesting

the modulatory action of 25-HC on the ISG pathways and broadening the innate immune response is enhanced in presence of a viral infection.

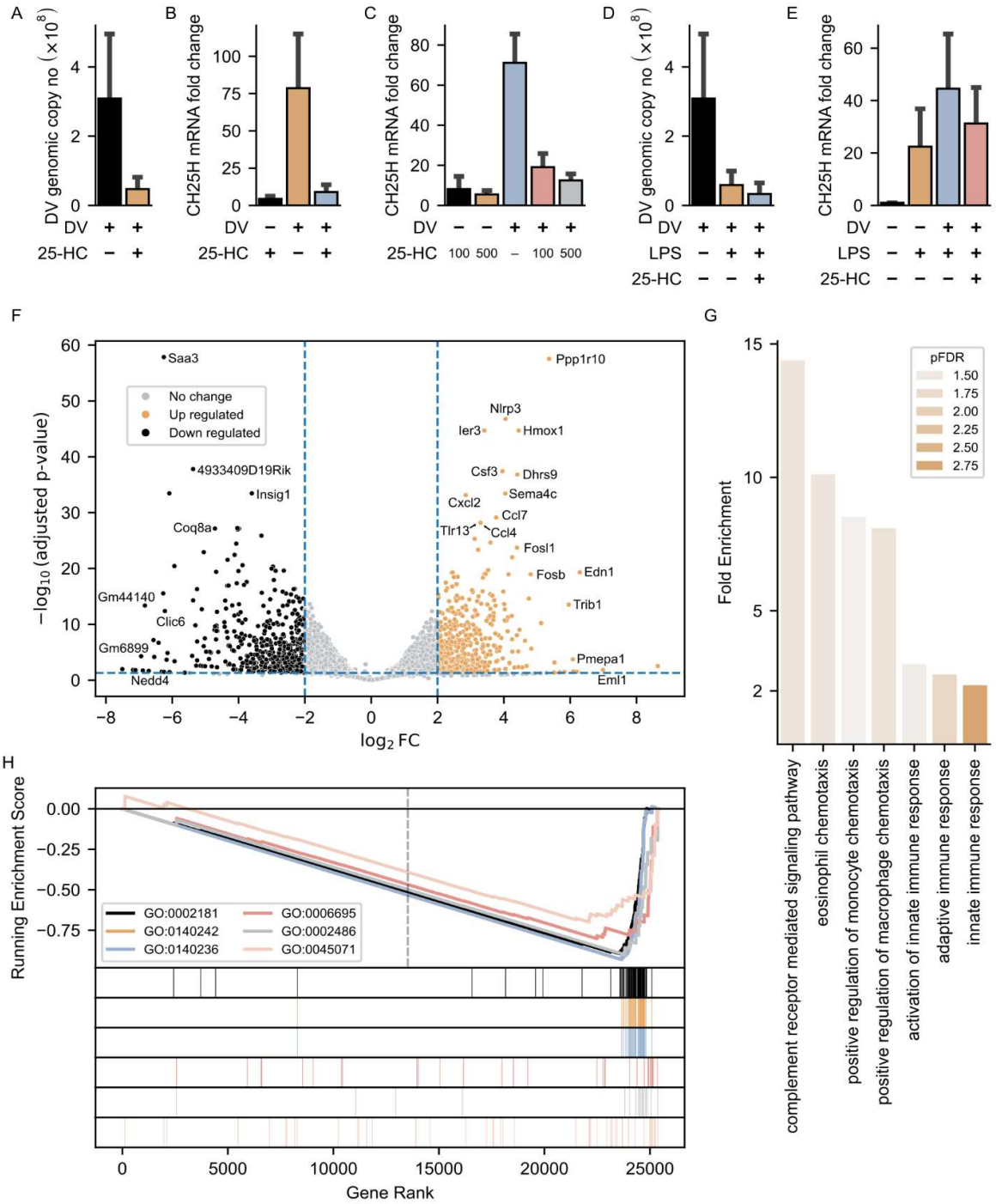

Figure 3:

A. Dengue virus genomic copy number in Raw cells following pre-incubation with 25-HC. Data presented as mean ± SEM (n=3)

B. CH25H gene expression normalized to β-actin in response to LPS treatment, with or without Dengue virus infection or 25-HC treatment, in Raw 264.7 cells. Data presented as mean ± SEM (n=3)

C. CH25H gene expression normalized to β-actin in response to Dengue virus infection under varying concentrations of 25-HC in Vero cells. Data presented as mean ± SEM (n=3)

D. Dengue virus genomic copy number in Raw cells following LPS pre-treatment. Data presented as mean ± SEM (n=3)

E. CH25H expression in Raw 264.7 cells in response to CV infection, 25-HC treatment, and LPS pre-treatment. Data presented as mean ± SEM (n=3)

F. Volcano plot showing the upregulation and downregulation of genes in Raw cells infected with Dengue virus and compared to pre-treated with 25-HC before infection.

G. GO enrichment analysis of significant genes in Raw cells infected with Dengue virus and pre-treated with 25-HC against only infected with Dengue virus.

H. Gene set enrichment analysis between Raw cells infected with Dengue virus after 25-HC pre-treatment vs Dengue virus infection only. Significantly downregulated pathways in Dengue virus after 25-HC pre-treatment as compared to Dengue virus only. FDR less than 0.05.

Modulation of cholesterol homeostasis and Immune response by 25-hydroxycholesterol during Dengue infection:

Another important class of gene expression changes observed in RNA-Seq was related to cholesterol homeostasis where key genes in cholesterol biosynthesis, transport, esterification and related regulatory genes were differently expressed. We observed that DENV infection results in upregulation of *SREBF2*, *HMGCR*, *SQLE* involved in cholesterol synthesis, indicating enhanced cholesterol synthesis (Figure 4A). However, Insig1 was also upregulated likely acting as a feedback regulator to control excess cholesterol by binding *SCAP* and preventing *SREBP* activation (Figure 4A). On the contrary, 25-HC, administered before Dengue Virus infection suppressed cholesterol biosynthesis pathway in several steps, downregulating *HMGCR*, *SREBF2*, and *SQLE* (Figure 4A). Notably, *SCAP* was upregulated upon pretreatment with 25-HC prior to DENV infection, suggesting a cellular feedback mechanism to limit cholesterol synthesis via *SREBF* inhibition. Our findings suggest that while 25-HC downregulates cholesterol biosynthesis, it promotes esterification of cholesterol by upregulation of *SOAT2*. Notably, *MSMO1*, *FAXDC2*, and *PID4* are strongly suppressed in 25-HC treated cells, indicating inhibition of sterol biosynthesis. These findings suggest that

25-HC modulates cholesterol homeostasis during Dengue virus infection, potentially limiting cholesterol availability required for viral replication. A schematic representation of the 25-HC-mediated modulation of the cholesterol biosynthesis pathway is provided in Figure 4B.

We investigated the impact of 25-hydroxycholesterol (25-HC) treatment on lipid droplet formation using lipid droplet-specific staining. Notably, incubation of cells with 25-HC resulted in a pronounced increase in lipid droplet abundance (Figure S2C) along with increase in *SOAT* gene expression (Figure S2 D).

25-HC has been reported to amplify proinflammatory responses in influenza virus infection by enhancing AP-1 recruitment and ER stress pathways [25]. However, our findings indicate a more complex role for 25-HC in DENV-induced immune responses in mouse macrophages. The Interferon Stimulated genes (ISGs), chemokine and cytokine expression profile observed in this study underscores the substantial immunomodulatory influence of 25-HC during Dengue virus infection. We observed that Interferon Stimulated Genes (ISGs) such as ISG15, *ISG20*, *IFITM* family, *Viperin* are robustly induced by Dengue Virus Infection and exhibited reduced expression upon 25-HC pre-treatment, suggesting a selective modulation or suppression of the interferon signalling pathway. Interestingly, pre-treatment with 25-HC has components of the AP-1 transcription factor family, particularly *Fos-b*, *Jun* and *Jund*, suggesting a selective activation of AP-1 dimers shown to amplify the general expression of general inflammatory mediators such as *IL36a*, *IL6*, *IL36g*, *TNF*, and several *CCL* chemokines (*CCL2*, *CCL3*, and *CCL4*).25-HC pretreatment significantly increased the expression of *NLRP3*, whereas expression of pro-inflammatory and apoptotic response such as *AIM2*, *Caspase 1*, *Caspase 3* is enhanced in Dengue virus infection resulting into production of cytokine such as *IL1b*, *IL18*.

However, the increased expression of CSF or anti-inflammatory cytokine such as *IL10* during 25-HC pretreatment suggests its role in modulating interferon signalling and inflammasome activation, underscoring a nuanced immune regulatory role for 25-HC during viral infections.

A proposed network model (Figure 4C) illustrates how 25-HC shifts the balance from excessive inflammation to a more controlled antiviral response, potentially improving both innate and adaptive immunity.

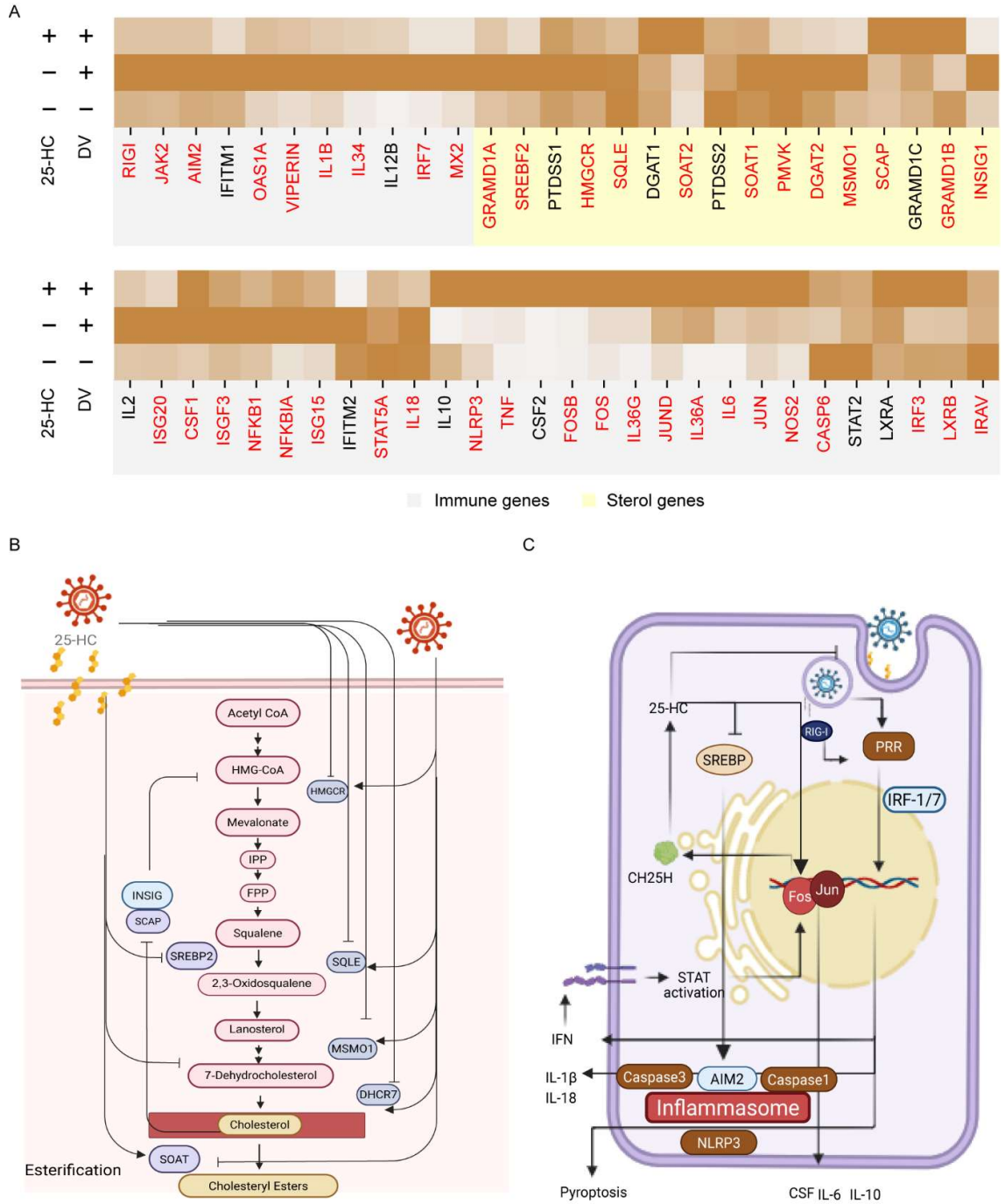

Figure 4. 25-HC Modulates Cholesterol Metabolism and Host Antiviral Immune Signalling in DENV-Infected Macrophages

A. Heatmap showing the relative expression of cholesterol biosynthesis genes (e.g., Hmgcr, Sqle, Srebf2, Dhcr7) and interferon-stimulated genes (ISGs) (e.g., Ifit1, Oas1a, Viperin, Stat1), and other immune response genes across three experimental conditions (n = 2). Expression values

are normalized to the highest expressed gene (value = 1); lighter shades indicate lower relative expression.

B. Schematic representation of the cholesterol biosynthesis pathway, highlighting key metabolic nodes modulated by DENV infection and 25-HC treatment. Red boxes denote metabolic intermediates; blunt-ended lines indicate inhibition; thin arrows represent upregulation.

C. Integrated schematic showing the effect of 25-HC on multiple antiviral immune signalling pathways during DENV infection. This includes activation of type I interferon responses via Stat1/Stat2, modulation of inflammasome components (Casp1, Il1b, Il18), suppression of proinflammatory interleukins (Il6, Csf, Il10), and regulation of the AP-1 complex (Jun, Fos-b). Black arrows denote canonical signalling pathways; green arrows indicate modulation by 25-HC.

Pathway insights of 25-HC and Synergy with Antiviral Combinations

Several antiviral agents have been shown to exhibit enhanced therapeutic effect when used in combination, surpassing the effects of individual drugs alone[26]. To identify the molecular pathway targeted by 25-hydroxycholesterol (25-HC), we selected known drugs with demonstrated anti-flaviviral activity to recognize that drug interactions can result in either enhancement or reduction in combined efficacy, as their interactions can influence the overall combined efficacy. Here, we evaluated the combination of 25-hydroxycholesterol with drugs targeting membrane fusion, (Picolinic acid) disrupt the acidic environment inside endosomes, (Chloroquine) or inhibit viral RNA replication (Remdesivir and small molecule K22 (N-{3-[4-(4-bromophenyl)-4-hydroxypiperidin-1-yl]-3-oxo-1-phenylprop-1-en-2-yl} benzamide), and assessed the synergistic effects of these combinations (see methods). The concentration of these drugs were tested in nine combinations of 25-HC with other drugs using a 3*3 dose matrix format.

It has been shown earlier that Remdesivir can inhibit RNA dependent RNA Polymerase (RdRps) from a broad class of RNA viruses ranging from Filoviridae, Coronaviridae, and Flaviriridae[39]. Small molecule K-22 showed anti-viral activity against different members of Flaviviradae, by inhibition of membrane-bound replication compartment biogenesis [40]. Chloroquine, an amine acido-tropic drug is reported to possess antiviral activities against RNA viruses such as SARS-CoV-2 by interfering with terminal glycosylation of the cellular receptor[41], Zika virus, Dengue virus by increasing endosomal pH [42]. We observed a synergistic interaction between 25-hydroxycholesterol (25-HC) and Remdesivir, resulting in a reduction in viral load that was up to 50% greater than the effect of each drug combined individually (Figure 4B). This drug pair showed the highest Bliss synergy (28.35%) and low

α value (0.02) (Figure 4D) corresponds to higher synergy in efficacy (Efficacy high due to less interaction between the drugs) Whether the combination of 25-HC and K-22 showed 30% more reduction in higher concentration of each drug. However, the combination of 25-HC and chloroquine shows pronounced synergy at higher concentration of both the drugs, reducing the viral load by 80% compared to combinational effect (Figure 4B). Both the combinations exhibit moderate bliss synergy (12.2% and 10.7%) respectively, with slightly higher α value (α=0.1 and α=0.09) reflecting stronger interactions contributing to combined efficacy.

Picolinic acid shows broad-spectrum anti-viral activity against enveloped viruses including SARS-CoV-2, Influenza A virus, and flaviviruses by inhibition of virus cellular membrane fusion and interfering with endocytosis [43].

The drug combination of 25-HC and Picolinic acid conferred dose-dependent suppression of virus infection, but there was no enhanced reduction while used in combination. However, this combination shows low bliss synergy (5.06%) but the highest alpha (α=0.41) indicating significant drug interaction effects. These results suggest that the strong interaction does not effectively enhance synergy, likely because both the drugs target same pathway of membrane fusion inhibition.

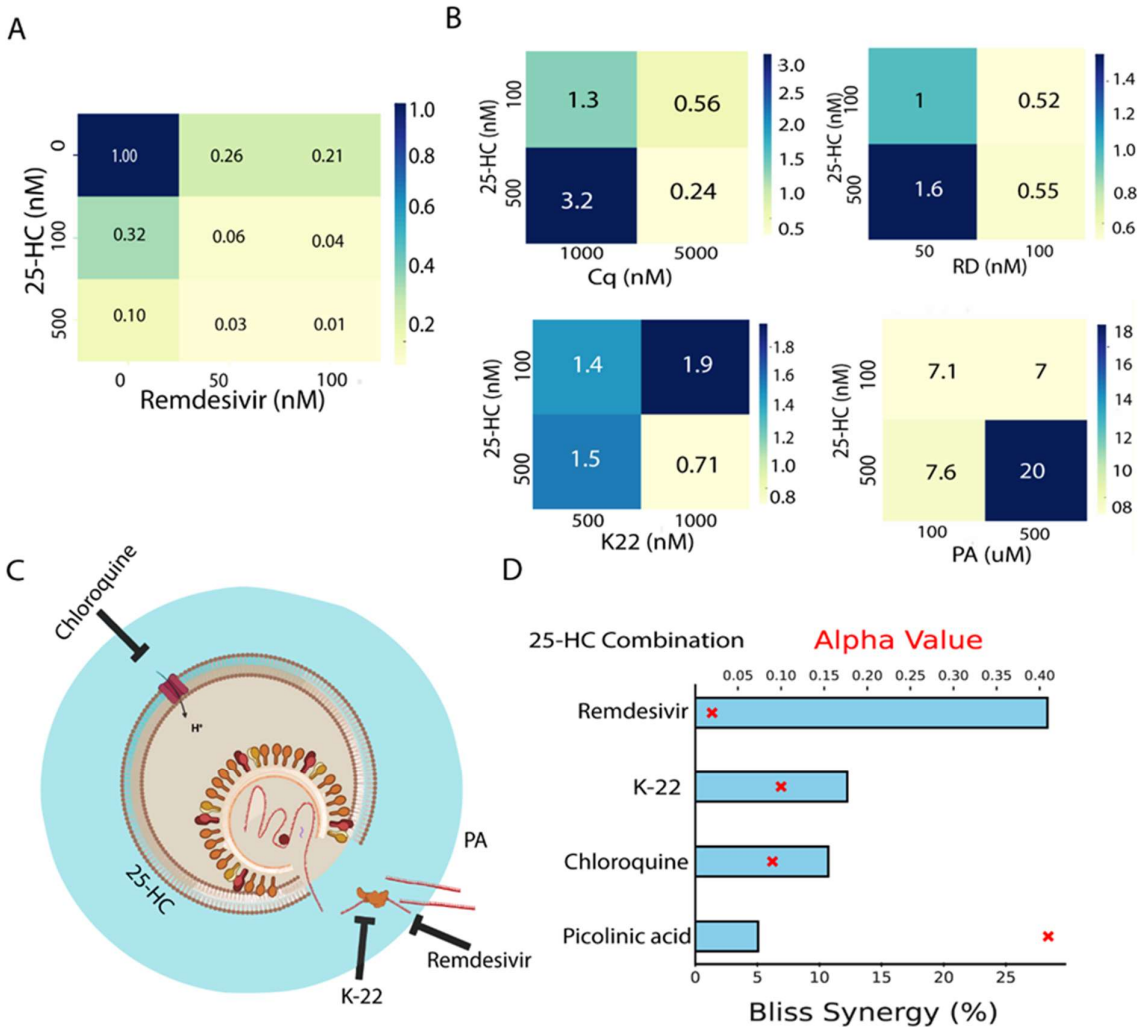

Figure 5: Investigation of the correlation between Chloroquine, K-22, Remdesivir, Picolinic acid, and 25-hydroxycholesterol (25-HC) in inhibiting virus infection.

A. Schematic representation illustrating how each drug inhibits virus infection at different stages of the viral lifecycle.
B. Bliss synergy scores and α values for the above drug combinations, quantifying their synergistic effects in inhibiting virus infection.
C. Virus copy number normalised to untreated control for the combination of Chloroquine and 25-HC
D. Comparative synergy between 25-HC and Chloroquine, Remdesivir, K-22, Picolinic acid for Vero cells.

Discussion:

The complex interaction between viral entry mechanisms and host response presents a critical regulatory checkpoint that can be exploited for antiviral intervention, as demonstrated by our findings on the inhibitory role of 25-HC in Dengue virus fusion. Time of addition assay showed 25-HC exerts dominant antiviral effect when added before infection. Dengue virus enters the cell by receptor mediated endocytosis followed by membrane fusion within the endosome, our in vitro liposome fusion assays confirmed a >2-fold reduction in lipid mixing and content mixing in pH 5 when 25-HC replaced even half of the cholesterol in target membranes (Figure 2A–D). The reduction is likely due to 25-HC directly interferes with the fusion process as 25-HC inserts into membranes at a different orientation than cholesterol [44], the 25-hydroxyl group interacts with phospholipid headgroups – leading to a less ordered, "thinner" bilayer. Such sterol-induced perturbations likely decrease the accessibility of cholesterol-rich microdomains that DENV needs for efficient endosomal fusion [45] as well with the finding that 25-HC inhibits SARS-Cov2 virus membrane fusion by depleting membrane accessible cholesterol [46].

To further investigate which early phase of Dengue virus infection is inhibited by 25-HC, our binding assay demonstrated that the presence of 25-HC in the target membrane significantly reduces the binding affinity of the E protein in vitro. The Dengue virus envelope (E) protein, which is essential for viral entry and fusion within the endosome [5] , exhibited diminished binding efficiency, likely due to alterations in membrane properties induced by 25-HC. We also found that 25-HC when present in the target membrane can reduce binding of the E protein in-Vitro.

It has previously been shown that *CH25H* is upregulated in macrophages by virus infection. Here we also found that Dengue virus infection in macrophages results in upregulation of JAK-STAT pathway, resulting in the enhancement of key Interferon Stimulated Genes (ISGs), whereas pre-treatment 25-HC attenuates such response. Our finding suggests that 25-HC can selectively modulate immune response, by upregulating AP1 transcription factors, Fos and Jun that is recruited on the AP1 site of the *csf* and *IL6* promoters as observed previously [25]. While 25-HC is produced downstream of virus infection, our finding demonstrates that its treatment before infection can modulate interferon responses and inflammatory activity, potentially limiting viral pathogenesis and inflammation.

25-hydroxycholesterol (25-HC) has been shown to inhibit non-enveloped viruses by promoting cholesterol esterification and lipid droplet formation, thereby restricting viral

replication [47]. Additionally, Dengue virus (DENV) uses lipid droplets (LDs) to replicate, therefore, DENV infected cells correlates with decrease in lipid droplets, which is required for efficient DENV replication [48]. Dengue virus (DENV) infection is known to disrupt cholesterol metabolism, while 25-hydroxycholesterol (25-HC) has been demonstrated to modulate this pathway [49], [50]. Similarly, we also observed modulation of cholesterol biosynthesis whereas 25-HC pre-treatment suppress this effect. We also observed that 25-HC pre-treatment downregulates *SREBP2*, a key gene in sterol synthesis and inflammasome oligomerization resulting in anti-inflammatory effect, it also results in down regulation of cholesterol biosynthesis pathway genes (*HMGCR*, *SQLE*), as a viral exploitation strategy. Examination of experimental condition with only 25-HC pre-treatment shows lesser variation in cholesterol biosynthetic pathway as well as stimulation of immune response.

The combinatorial analysis of 25-HC and established anti-influenza drugs, conducted using mathematical model, provided valuable insights into the involved pathways. The best outcome was observed between 25-HC and Remdesivir that implies lesser inhibition of RDRP complex [39]. However, the high alpha value between 25-HC and Picolinic acid indicate significant drug interaction between them probably because both the drugs target the same pathway of membrane fusion inhibition[43]. We tested these drugs at concentrations, one of them higher than IC50, it was non-toxic for cells.

This study uniquely bridges the traditionally distinct domains of membrane biophysics and cellular and molecular biology to elucidate how 25-HC inhibits Dengue virus infection. By developing an in vitro bulk fusion assay, we captured the real-time mixing of viral membranes with liposomes under varying conditions, providing a mechanistic view of sterol-mediated membrane perturbations. In parallel, we employed transcriptomic (mRNA-seq) analysis in a cell culture system to map the downstream gene expression responses triggered by 25-HC. We also integrated image-based quantification of viral load, enabling precise assessment of infection dynamics. Furthermore, we developed a model based on established mathematical frameworks to quantify the synergistic effects of drug combinations, offering a predictive tool for therapeutic optimization. The integration of these diverse methodologies—spanning biophysics, bioinformatics, and quantitative modelling—represents a novel, interdisciplinary approach that advances our understanding of host-directed antiviral strategies. While our experiments establish in vitro efficacy, the translation of these effects to in vivo models remains uncertain. While our gene expression analysis is based on mRNA sequencing, further investigation at the protein level is crucial for a complete understanding

of the observed changes. The bioavailability and stability of 25-HC also present challenges, as its cholesterol-derived structure may impact its solubility and delivery in therapeutic applications. Furthermore, the use of a reverse genetics-derived Dengue Virus 2 strain propagated and purified in vitro constrains the interpretation of our results to this specific strain. Studies using clinical isolates of various dengue serotypes are therefore essential to validate and extend these observations Additionally, as an oxysterol involved in immune regulation, 25-HC may have broader immunomodulatory effects that could influence host-pathogen interactions in ways not yet fully understood.

Overall, this study establishes 25-HC as a potential inhibitor of Dengue Virus infection with promising modulation of membrane properties, lipid metabolism and immune response

Conclusion: Leveraging Dengue virus infection as a model, our study demonstrates that 25-hydroxycholesterol (25-HC) functions as a potent, multi-faceted antiviral through its complex perturbation of viral entry, modulation of cholesterol metabolism, and orchestration of immune signalling pathways. By integrating membrane biophysics with transcriptomic profiling, we provide a systems-level understanding of how 25-HC not only prevents viral infection but also fine-tunes antiviral cellular responses to mitigate hyperinflammation. Notably, our findings highlight that pre-existing 25-HC levels can precondition cells by inducing metabolic adaptations that enhance innate immune responses, regulate cytokine-chemokine dynamics, and reprogram lipid-associated antiviral defence mechanisms.

[1] M. S. Diamond and T. C. Pierson, “Molecular Insight into Dengue Virus Pathogenesis and Its Implications for Disease Control,” Aug. 01, 2015, *Cell Press*. doi: 10.1016/j.cell.2015.07.005.

[2] S. C. Harrison, “Viral membrane fusion,” May 01, 2015, *Academic Press Inc.* doi: 10.1016/j.virol.2015.03.043.

[3] S. C. Harrison, “Viral membrane fusion,” Jul. 2008. doi: 10.1038/nsmb.1456.

[4] P. C. Y. Woo, Y. Huang, S. K. P. Lau, and K. Y. Yuen, “Coronavirus genomics and bioinformatics analysis,” 2010, *MDPI AG*. doi: 10.3390/v2081803.

[5] Y. Modis, S. Ogata, D. Clements, and S. C. Harrison, “Structure of the dengue virus envelope protein after membrane fusion,” 2004. [Online]. Available: www.nature.com/nature

[6] A. C. Walls, Y. J. Park, M. A. Tortorici, A. Wall, A. T. McGuire, and D. Veesler, “Structure, Function, and Antigenicity of the SARS-CoV-2 Spike Glycoprotein,” *Cell*, vol. 181, no. 2, pp. 281-292.e6, Apr. 2020, doi: 10.1016/j.cell.2020.02.058.

[7] V. A. Kostyuchenko *et al.*, “Structure of the thermally stable Zika virus,” *Nature*, vol. 533, pp. 425–428, Apr. 2016, doi: 10.1038/nature17994.

[8] J. Mercer, M. Schelhaas, and A. Helenius, “Virus entry by endocytosis,” Jul. 07, 2010. doi: 10.1146/annurev-biochem-060208-104626.

[9] J. M. Shim, J. Kim, T. Tenson, J. Y. Min, and D. E. Kainov, “Influenza virus infection, interferon response, viral counter-response, and apoptosis,” Aug. 12, 2017, *MDPI AG*. doi: 10.3390/v9080223.

[10] E. Zaitseva, S. T. Yang, K. Melikov, S. Pourmal, and L. V. Chernomordik, “Dengue virus ensures its fusion in late endosomes using compartment-specific lipids,” *PLoS Pathog*, vol. 6, no. 10, Oct. 2010, doi: 10.1371/journal.ppat.1001131.

[11] R. Zang *et al.*, “Cholesterol 25-hydroxylase suppresses SARS-CoV-2 replication by blocking membrane fusion”, doi: 10.1073/pnas.2012197117/-/DCSupplemental.

[12] B. Gomes, S. Gonçalves, A. Disalvo, A. Hollmann, and N. C. Santos, “Effect of 25-hydroxycholesterol in viral membrane fusion: Insights on HIV inhibition,” *Biochim Biophys Acta Biomembr*, vol. 1860, no. 5, pp. 1171–1178, May 2018, doi: 10.1016/j.bbamem.2018.02.001.

[13] Y. Chen *et al.*, “Interferon-inducible cholesterol-25-hydroxylase inhibits hepatitis C virus replication via distinct mechanisms,” *Sci Rep*, vol. 4, Dec. 2014, doi: 10.1038/srep07242.

[14] V. Cagno *et al.*, “Inhibition of herpes simplex-1 virus replication by 25-hydroxycholesterol and 27-hydroxycholesterol,” *Redox Biol*, vol. 12, pp. 522–527, Aug. 2017, doi: 10.1016/j.redox.2017.03.016.

[15] A. Civra *et al.*, “25-Hydroxycholesterol and 27-hydroxycholesterol inhibit human rotavirus infection by sequestering viral particles into late endosomes,” *Redox Biol*, vol. 19, pp. 318–330, Oct. 2018, doi: 10.1016/j.redox.2018.09.003.

[16] E. G. Lund, T. A. Kerr, J. Sakai, W.-P. Li, and D. W. Russell, “cDNA Cloning of Mouse and Human Cholesterol 25-Hydroxylases, Polytopic Membrane Proteins That Synthesize a Potent Oxysterol Regulator of Lipid Metabolism*,” 1998. [Online]. Available: http://www.jbc.org

[17] S. Y. Liu *et al.*, “Interferon-Inducible Cholesterol-25-Hydroxylase Broadly Inhibits Viral Entry by Production of 25-Hydroxycholesterol,” *Immunity*, vol. 38, no. 1, pp. 92–105, Jan. 2013, doi: 10.1016/j.immuni.2012.11.005.

[18] D. R. Bauman, A. D. Bitmansour, J. G. Mcdonald, B. M. Thompson, G. Liang, and D. W. Russell, “25-Hydroxycholesterol secreted by macrophages in response to Toll-like receptor activation suppresses immunoglobulin A production.” [Online]. Available: www.pnas.org/cgi/content/full/

[19] M. Blanc *et al.*, “The Transcription Factor STAT-1 Couples Macrophage Synthesis of 25-Hydroxycholesterol to the Interferon Antiviral Response,” *Immunity*, vol. 38, no. 1, pp. 106–118, Jan. 2013, doi: 10.1016/j.immuni.2012.11.004.

[20] A. Reboldi, E. V. Dang, J. G. McDonald, G. Liang, D. W. Russell, and J. G. Cyster, “25-hydroxycholesterol suppresses interleukin-1-driven inflammation downstream of type I interferon,” *Science (1979)*, vol. 345, no. 6197, pp. 679–684, Aug. 2014, doi: 10.1126/science.1254790.

[21] Y. Liu *et al.*, “Activation of liver X receptor plays a central role in antiviral actions of 25-hydroxycholesterol,” *J Lipid Res*, vol. 59, no. 12, pp. 2287–2296, 2018, doi: 10.1194/jlr.M084558.

[22] J. D. Horton, J. L. Goldstein, and M. S. Brown, “SREBPs: activators of the complete program of cholesterol and fatty acid synthesis in the liver,” *Journal of Clinical Investigation*, vol. 109, no. 9, pp. 1125–1131, May 2002, doi: 10.1172/jci200215593.

[23] H. Merta *et al.*, “Spatial proteomics of ER tubules reveals CLMN, an ER-actin tether at focal adhesions that promotes cell migration,” *Cell Rep*, vol. 44, no. 4, p. 115502, Apr. 2025, doi: 10.1016/j.celrep.2025.115502.

[24] X. Y. Dong, S. Q. Tang, and J. D. Chen, “Dual functions of Insig proteins in cholesterol homeostasis,” Dec. 18, 2012, *BioMed Central Ltd.* doi: 10.1186/1476-511X-11-173.

[25] E. S. Gold *et al.*, “25-Hydroxycholesterol acts as an amplifier of inflammatory signaling,” *Proc Natl Acad Sci U S A*, vol. 111, no. 29, pp. 10666–10671, Jul. 2014, doi: 10.1073/pnas.1404271111.

[26] S. Einav, H. Dvory-Sobol, E. Gehrig, and J. S. Glenn, “The Hepatitis C virus (HCV) NS4B RNA binding inhibitor clemizole is highly synergistic with HCV protease inhibitors,” *Journal of Infectious Diseases*, vol. 202, no. 1, pp. 65–74, Jul. 2010, doi: 10.1086/653080.

[27] R. M. Kinney *et al.*, “ARTICLE NO. VY978500 and †Center for Vaccine Development, Institute of Science and Technology for Development, Mahidol University at Salaya, 25/25 Phutthamonthon 4,” 1997.

[28] A. Dobin *et al.*, “STAR: Ultrafast universal RNA-seq aligner,” *Bioinformatics*, vol. 29, no. 1, pp. 15–21, Jan. 2013, doi: 10.1093/bioinformatics/bts635.

[29] Y. Liao, G. K. Smyth, and W. Shi, “FeatureCounts: An efficient general purpose program for assigning sequence reads to genomic features,” *Bioinformatics*, vol. 30, no. 7, pp. 923–930, Apr. 2014, doi: 10.1093/bioinformatics/btt656.

[30] B. Muzellec, M. Teleńczuk, V. Cabeli, and M. Andreux, “PyDESeq2: a python package for bulk RNA-seq differential expression analysis,” *Bioinformatics*, vol. 39, no. 9, Sep. 2023, doi: 10.1093/bioinformatics/btad547.

[31] A. Sannigrahi, V. H. Rai, M. V. Chalil, D. Chakraborty, S. K. Meher, and R. Roy, “A Versatile Suspended Lipid Membrane System for Probing Membrane Remodeling and Disruption,” *Membranes (Basel)*, vol. 12, no. 12, Dec. 2022, doi: 10.3390/membranes12121190.

[32] A. Sannigrahi *et al.*, “Leishmania protein KMP-11 modulates cholesterol transport and membrane fluidity to facilitate host cell invasion.,” *EMBO Rep*, Oct. 2024, doi: 10.1038/s44319-024-00302-7.

[33] A. Sannigrahi *et al.*, “The metal cofactor zinc and interacting membranes modulate sod1 conformation-aggregation landscape in an in vitro als model,” *Elife*, vol. 10, Apr. 2021, doi: 10.7554/ELIFE.61453.

[34] C. Li *et al.*, “25-Hydroxycholesterol Protects Host against Zika Virus Infection and Its Associated Microcephaly in a Mouse Model,” *Immunity*, vol. 46, no. 3, pp. 446–456, Mar. 2017, doi: 10.1016/j.immuni.2017.02.012.

[35] A. M. Villamil Giraldo, S. Mannsverk, and P. M. Kasson, “Measuring single-virus fusion kinetics using an assay for nucleic acid exposure,” *Biophys J*, vol. 121, no. 23, pp. 4467–4475, Dec. 2022, doi: 10.1016/j.bpj.2022.11.002.

[36] M. E. Abrams *et al.*, “Oxysterols provide innate immunity to bacterial infection by mobilizing cell surface accessible cholesterol,” *Nat Microbiol*, vol. 5, no. 7, pp. 929–942, Jul. 2020, doi: 10.1038/s41564-020-0701-5.

[37] H. M. van der Schaar *et al.*, “Characterization of the Early Events in Dengue Virus Cell Entry by Biochemical Assays and Single-Virus Tracking,” *J Virol*, vol. 81, no. 21, pp. 12019–12028, Nov. 2007, doi: 10.1128/jvi.00300-07.

[38] C. Fernandes-Santos and E. L. de Azeredo, “Innate Immune Response to Dengue Virus: Toll-like Receptors and Antiviral Response,” May 01, 2022, *MDPI*. doi: 10.3390/v14050992.

[39] E. Konkolova *et al.*, “Remdesivir triphosphate can efficiently inhibit the RNA-dependent RNA polymerase from various flaviviruses,” *Antiviral Res*, vol. 182, Oct. 2020, doi: 10.1016/j.antiviral.2020.104899.

[40] O. García-Nicolás *et al.*, “The Small-Compound Inhibitor K22 Displays Broad Antiviral Activity against Different Members of the Family Flaviviridae and Offers Potential as a Panviral Inhibitor,” 2018. [Online]. Available: https://doi.org/10

[41] M. J. Vincent *et al.*, “Chloroquine is a potent inhibitor of SARS coronavirus infection and spread,” *Virol J*, vol. 2, Aug. 2005, doi: 10.1186/1743-422X-2-69.

[42] K. J. S. Farias, P. R. L. Machado, R. F. de Almeida Junior, A. A. de Aquino, and B. A. L. da Fonseca, “Chloroquine interferes with dengue-2 virus replication in U937 cells,” *Microbiol Immunol*, vol. 58, no. 6, pp. 318–326, 2014, doi: 10.1111/1348-0421.12154.

[43] R. Narayan *et al.*, “Picolinic acid is a broad-spectrum inhibitor of enveloped virus entry that restricts SARS-CoV-2 and influenza A virus in vivo,” *Cell Rep Med*, vol. 4, no. 8, Aug. 2023, doi: 10.1016/j.xcrm.2023.101127.

[44] M. M. Domingues, B. Gomes, A. Hollmann, and N. C. Santos, “25-hydroxycholesterol effect on membrane structure and mechanical properties,” *Int J Mol Sci*, vol. 22, no. 5, pp. 1–12, Mar. 2021, doi: 10.3390/ijms22052574.

[45] R. Soto-Acosta *et al.*, “The increase in cholesterol levels at early stages after dengue virus infection correlates with an augment in LDL particle uptake and HMG-CoA reductase activity,” *Virology*, vol. 442, no. 2, pp. 132–147, Aug. 2013, doi: 10.1016/j.virol.2013.04.003.

[46] S. Wang *et al.*, “ Cholesterol 25-Hydroxylase inhibits SARS -CoV-2 and other coronaviruses by depleting membrane cholesterol ,” *EMBO J*, vol. 39, no. 21, Nov. 2020, doi: 10.15252/embj.2020106057.

[47] J. L. Zhang, X. F. Wang, J. L. Li, C. Duan, and J. F. Wang, “The cholesterol metabolite 25-hydroxycholesterol suppresses porcine deltacoronavirus via lipophagy inhibition and mTORC1 modulation,” *Vet Res*, vol. 56, no. 1, p. 23, Jan. 2025, doi: 10.1186/s13567-025-01452-9.

[48] N. S. Heaton and G. Randall, “Dengue virus-induced autophagy regulates lipid metabolism,” *Cell Host Microbe*, vol. 8, no. 5, pp. 422–432, Nov. 2010, doi: 10.1016/j.chom.2010.10.006.

[49] C. Nguyen, J. Saint-Pol, S. Dib, C. Pot, and F. Gosselet, “25-Hydroxycholesterol in health and diseases,” Jan. 01, 2024, *American Society for Biochemistry and Molecular Biology Inc.* doi: 10.1016/j.jlr.2023.100486.

[50] M. S. Lee and S. J. Bensinger, “Reprogramming cholesterol metabolism in macrophages and its role in host defense against cholesterol-dependent cytolysins,” Mar. 01, 2022, *Springer Nature*. doi: 10.1038/s41423-021-00827-0.